Article

Not peer-reviewed version

Compensation Function Observer-based Backstepping Sliding Mode Control of Uncertain Electro-hydraulic Servo Systems

Changzhong Pan *, Yanjun Wang , Simon X. Yang , Zhijing Li , Jinsen Xiao

Posted Date: 4 September 2024

doi: 10.20944/preprints202409.0319.v1

Keywords: Lyapunov function; electro-hydraulic servo system; compensation function observer (CFO); backstepping; sliding mode control; observer-based control

 doi:10.20944/preprints202409.0319.v1

Article

Compensation Function Observer-based Backstepping Sliding Mode Control of Uncertain Electro-Hydraulic Servo Systems

Changzhong Pan [1,2,*], Yanjun Wang [1], Simon X. Yang [3], Zhijing Li [1] and Jinsen Xiao [4]

[1] School of Information and Electrical Engineering, Hunan University of Science and Technology, Xiangtan 411201, China
[2] School of Automation, Guangdong University of Petrochemical Technology, Maoming 525000, China
[3] School of Engineering, University of Guelph, Guelph, Ontario N1G 2W1, Canada
[4] Department of Mathematics, Guangdong University of Petrochemical Technology, Maoming 525000, China
* Correspondence: pancz@hnust.edu.cn

Abstract: Observer-based control is the most commonly used method in the control of electro-hydraulic servo system (EHSS) with uncertainties, but it suffers from the drawback of low accuracy under the influence of large external load forces and disturbances. To address this problem, this paper proposes a novel compensation function observer-based backstepping sliding mode control (BSMC) approach to achieve high-accuracy tracking control. In particular, the model uncertainties, including nonlinearities, parameter perturbations and external disturbances are analyzed and treated together as a lumped disturbance. Then, a fourth-order compensation function observer (CFO) is constructed, which fully utilizes the system state information to accurately estimate the lumped disturbance. On this basis, the estimate of the lumped disturbance is incorporated into the design of an backstepping sliding mode controller, allowing the control system to compensate for the disturbance effect. The stability of the closed-loop control system under the CFO and BSMC is rigorously proven through the use of Lyapunov theory, which guarantees that all the tracking error signals converge exponentially to the origin. Comparative simulations are carried out to show the effectiveness and efficiency of the proposed approach, i.e., compared with PID and ESO-based BSMC methods, the tracking accuracy is improved by 99.93% and 99.76%, respectively.

Keywords: lyapunov function; electro-hydraulic servo system; compensation function observer (CFO); backstepping; sliding mode control; observer-based control

1. Introduction

As a complex nonlinear mechatronic system, electro-hydraulic servo system (EHSS) possesses many prominent merits such as fast response, strong load capacity, high power-to-weight ratio and so on [1–3]. Because of these advantages, EHSS has been extensively used in modern industrial applications, such as digging robots [4–6], hydraulic press [7,8], and mechanical arms [9,10], etc. Nevertheless, the EHSS in practical applications always suffers from various uncertainties. On one hand, the model parameters such as load mass, effective oil bulk modulus, leakage coefficient may significantly change with working conditions, temperature and equipment wear. On the other hand, the hydraulic system has strong nonlinearities in the flow and pressure dynamics of the control valve, oil compressibility, and leakage. Furthermore, owing to the intricacy of working environment, the EHSS is inevitably susceptible to unknown external load forces and disturbances. All these uncertainties could seriously deteriorate the system control performance, or even destroy the system. Therefore, the high-precision tracking control of EHSS in the presence of uncertainties with advanced control methods still poses challenges for engineers.

Over the past decades, there have been remarkable advancements on the control of EHSS. The existing control methods can be classified into three categories: *linear control* [11–17], *nonlinear control* [18–34], and *observer-based control* [37–44].

 doi:10.20944/preprints202409.0319.v1

The linear control algorithms, which are developed using conventional PID [11–14] or feedback linearization techniques [15–17], are simple and easy to implement in engineering. However, they only perform well under certain operating conditions, and fail to achieve satisfactory performance in the presence of aforementioned uncertainties including parameter permutations, nonlinearities and disturbances. To enhance the control performance of EHSS, extensive research has been conducted, and numerous advanced nonlinear control methods have been proposed, such as backstepping control, adaptive control, sliding model control and so on.

The backstepping technique is one of the most powerful tools in nonlinear control, in which the control laws are designed recursively by constructing a serious of control Lyapunov functions. The distinctive feature of this approach lies in its well-defined step-by-step design procedure, and the system stability can be rigorously guaranteed by a Lyapunov stability theory. However, the control laws designed by this method depends on the accurate model of the system. To remove this obstacle, researchers often combine it with other advanced control methods such as adaptive control, fuzzy logic system (FLS)/neural network (NN) and sliding mode control (SMC). For example, a desired compensation adaptive control framework was proposed in [18,19], where a projection-type adaptive law was designed to estimate the unknown parameters. In [20], an adaptive robust controller was developed by combining adaptive robust control with a discrete disturbance estimator, which can compensate for unknown parameters, nonlinearities and external disturbances. Unfortunately, the adaptive design process is usually required to be linearly parameterized with unknown constant parameters, which is not always satisfied for the complex EHSS. By employing FLS to approximate nonlinearities, parameter uncertainties and external disturbances, adaptive fuzzy backstepping controllers were presented in [21–24]. Similarly, taking advantage of the universal approximation ability of NN, adaptive backstepping NN control schemes have been extensively proposed in [25–27]. However, the control algorithms using FLS/NN are usually computationally expensive, since FLS relies heavily on the knowledge rules of expert and NN requires either on-line learning or off-line training procedures to make the controller perform properly.

SMC is famous for its insensitivity to uncertainties in the manner of constructing a sliding mode surface. Once the system states reach the surface, the controller has strong robustness against uncertainties. In view of this excellent feature, several control strategies that combine backstepping and SMC have been proposed in [28–31] to improve the robustness of EHSS with backlash links, non-structural uncertainties or dead-zones. Furthermore, by incorporating NNs, adaptive NN sliding mode control approaches were presented in [32–34] for EHSS to achieve a high tracking accuracy.

Observer-based control has been proved to be a powerful technique to address uncertainties. The basic idea of this methodology is to design an observer to estimate the uncertainties and compensate for the effect in the control loop. Typical observers include high-gain observer (HGO), nonlinear disturbance observer (NDO), adaptive observer (AO), sliding mode observer (SMO), and extended state observer (ESO). Among them, ESO is the most classical disturbance estimation method, which regards the internal and external disturbance of the system as an extended system state variable [35,36]. In [37–39], three ESO-based sliding model controllers are proposed for EHSS, in which ESO is used to estimate the lumped disturbance while the convergence of the system state is guaranteed by SMC technique. In addition, employing ESO with backstepping, a variety of control strategies such as ESO-based finite-time backstepping control [40,41], ESO-based adaptive backstepping control [42], and ESO-based backstepping robust control [43,44], have been proposed. Nevertheless, the ESO still has some drawbacks in the estimation accuracy and system convergence. It has been verified in [45] that the structure of ESO can be equivalent to a Type-I tracking system, which means zero steady-state error convergence can only be achieved in the presence of constant disturbances.

According to the above literature review and analysis, it is evident that ESO-based control combined with SMC in the framework of backstepping is the most powerful and effective method for the control of EHSS in the presence of complex nonlinearities and uncertainties. However, the dynamics and disturbances of EHSS are dynamically changing, i.e., they are not constant. When

 doi:10.20944/preprints202409.0319.v1

employing the ESO-based backstepping sliding model control method, it faces challenging problems of low estimation accuracy and big estimation lag. Although increasing the ESO gains may improve the estimation accuracy, it would also amplify noises, leading to the so-called peaking phenomenon [46,47], or even system instability. Therefore, the improved backstepping SMC design based on the observer to handle this issue still needs further investigation. Recently, a novel compensation function observer (CFO) with a pure integral structure was proposed by Qi et al. in [45]. By introducing velocity information and using a first-order filter or integrator as a compensation function, the CFO becomes a Type-III system, which enable it to estimate constant, slope and acceleration disturbances or uncertainties below with zero steady-state error. Due to these advantages, CFO was extensively applied to the attitude control of quadrotor aircraft [48,49], yielding favorable control outcomes. However, the application of CFO on EHSS has not been reported.

Motivated by the above observations, this paper exploits a novel CFO-based backstepping sliding model control (CFO-BMSC) approach to enhance the tracking accuracy of EHSS subjected to various uncertainties. The nonlinearities and disturbances of EHSS are first analyzed, and the model equation is rearranged as a appropriate form, where all the uncertainties affecting the system including unknown frictions, parameter perturbations and external disturbances are collectively treated as a lumped disturbance. Then, inspired by the unique feature of compensation function, a fourth-order CFO is employed to estimate the lumped disturbance accurately, which is in turn incorporated into the control design to compensate for the effect of the disturbance. Furthermore, in the framework of backstepping, a sliding model controller is designed to stabilize all the tracking errors. The primary features and contributions of the proposed approach are underlined as follows.

(1) Different from previous ESO-based methods (e.g., [37,40,41,43]), the CFO adopts a Type-III structure and fully utilizes system state information, which make it capable of estimating the disturbance with higher estimation accuracy. Detailed comparisons between the performance of ESO and CFO in estimation of different disturbances are examined by extensive comparison simulations.
(2) In comparison with conventional PID and ESO-based BSMC [12,47], the proposed CFO-BMSC tracks the reference trajectory with no phase lag under the influence of large external load forces and disturbances, and the tracking accuracy is increased by 99.93% and 99.76% respectively, obtaining better transient and steady-state tracking performances. To our best knowledge, this is the first attempt to incorporate CFO into the backstepping sliding mode control of EHSS.
(3) The stability of the overall system including the CFO and BSMC is rigorously analyzed by Lyapunov stability theory, which guarantees that the closed-loop control system is exponentially stable, and the tracking errors converge to the origin.

The remainder of this paper is organized as follows. The nonlinear mathematical model of the EHSS under study is given in Section 2. The control system design including compensation function observer, sliding mode backstepping controller, and the system stability analysis are presented in Section 3. Simulation results with comparisons are shown in Section 4, and conclusion remarks are finally given in Section 5.

2. System Modeling and Problem Description

Figure 1 is the working principle diagram of the electro-hydraulic servo system (EHSS), which is consisted of an electro-hydraulic servo valve and a hydraulic cylinder. The load is controlled by an electro-hydraulic servo valve, which converts the received electrical signal into a hydraulic signal, and then drive the hydraulic cylinder. For the considered EHSS in Figure 1, m is the mass of the load, A is the ram area of the chamber, x_p is the piston displacement, x_v is the servo valve spool displacement, f_d is the unmodeled friction and unknown disturbances in the systems, P_1 is the pressure inside the left chamber of the hydraulic cylinder, P_2 is the pressure inside the right chamber of the hydraulic cylinder, Q_1 is the supplied flow rate to the two chambers, Q_2 is the return flow rate to the two chambers, P_s is the supply pressure.

 doi:10.20944/preprints202409.0319.v1

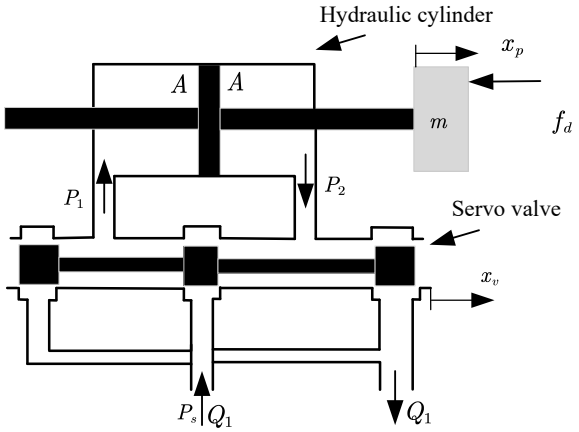

Figure 1. Schematic diagram of electro-hydraulic servo system.

According to Newton's second law, the dynamic equation of the hydraulic cylinder is

$$P_L A = m\ddot{x}_p + B\dot{x}_p + f_d, \tag{1}$$

where P_L is the load pressure in the hydraulic actuator, $P_L = P_1 - P_2$; B is the coefficient of the viscous friction force. Considering the effect of internal leakages, the load pressure dynamics can be defined as [19]

$$\dot{P}_L = \frac{4\beta_e}{V_t}\left(Q_L - A\dot{x}_p - C_t P_L\right), \tag{2}$$

where β_e is the effective oil bulk modulus; Q_L is the load flow, $Q_L = \frac{1}{2}(Q_1 + Q_2)$; C_t is the coefficient of the total internal leakage of the hydraulic cylinder.

Given that the response of the servo valve is much higher than the hydraulic cylinder, the relationship between the spool displacement and the control input is approximated as $x_v = k_i u$, where k_i is a positive constant. The load flow can be obtained [19]

$$Q_L = k_t u\sqrt{P_S - P_L \mathrm{sign} u}, \tag{3}$$

where k_t is the flow gain, $k_t = k_i C_d\sqrt{\frac{2}{\rho}}$, C_d is the flow coefficient, ω is the area gradient of the servo valve, ρ is the oil density.

Define $x = [x_1, x_2, x_3]^T = [x_p, \dot{x}_p, \ddot{x}_p]^T$ as the state variables, then from (1)-(3), the state-space equation of the EHSS is expressed as

$$\begin{cases} \dot{x}_1 = x_2, \\ \dot{x}_2 = x_3, \\ \dot{x}_3 = R_1 x_2 + R_2 u + F, \end{cases} \tag{4}$$

where

$$\begin{aligned} R_1 &= -\frac{4A^2\beta_e}{mV_t} + \frac{B^2}{m^2}, \\ R_2 &= \frac{4A\beta_e k_t}{mV_t}\sqrt{P_S - P_L \mathrm{sign} u}, \\ F &= \varphi P_L - \frac{B}{m} f_d + \dot{f}_d, \\ \varphi &= -\frac{4A\beta_e C_t}{mV_t} - \frac{BA}{m^2}. \end{aligned} \tag{5}$$

Note that R_1 and R_2 are certain constants, both of which are related to the system parameters. In practice, it is often difficult to obtain accurate system parameters, so there exist uncertain parts for R_1

 doi:10.20944/preprints202409.0319.v1

and R_2, which can be denoted as ΔR_1 and ΔR_2. The term F includes unmodeled dynamics such as frictions and unknown external disturbances. In this paper, all the mentioned uncertainties are treated as a lumped disturbance f_u, which can be expressed as

$$f_u = \Delta R_1 x_2 + \Delta R_2 u + F. \tag{6}$$

Thus, the Equation (4) is rewritten as

$$\begin{cases} \dot{x}_1 = x_2, \\ \dot{x}_2 = x_3, \\ \dot{x}_3 = f_k + R_2 u + f_u, \end{cases} \tag{7}$$

where $f_k = R_1 x_2$ is the known nominal part of the EHSS model, and f_u is the unknown lumped disturbance. In this paper, an CFO is designed to estimate f_u in real time, and the estimate value is fed back to the controller to compensate for the effect of f_u such that the output x_1 can track the desired trajectory x_d quickly and accurately.

3. Control Design

In this sction, an overview of the structure of the proposed control scheme is first presented and described. Then, a compensation function observer (CFO) is designed to accurately estimate the lumped disturbance in real time, on the basis of which a backstepping sliding mode controller is designed to achieve the trajectory tracking control.

3.1. Structure of the Proposed Hierarchical Control Scheme

Figure 2 shows the structure of the proposed hierarchical backstepping sliding mode control scheme based on CFO for the EHSS with uncertainties. By using the backstepping method for the EHSS model, the present control strategy is divided into two control loops, which are named as *virtual control loop* and *actual control loop*. In the virtual control loop, the goal is to design virtual control laws x_{2d} and x_{3d} to ensure x_1 tracks x_d ideally, while in the *actual control loop*, it aims to design a final control law to stabilize the tracking errors of intermediate variables. By taking the unknown lumped disturbance into consideration, a novel CFO is adopted in the actual loop to provide a real-time accurate estimate $\hat{x}_4$ of the lumped disturbance.

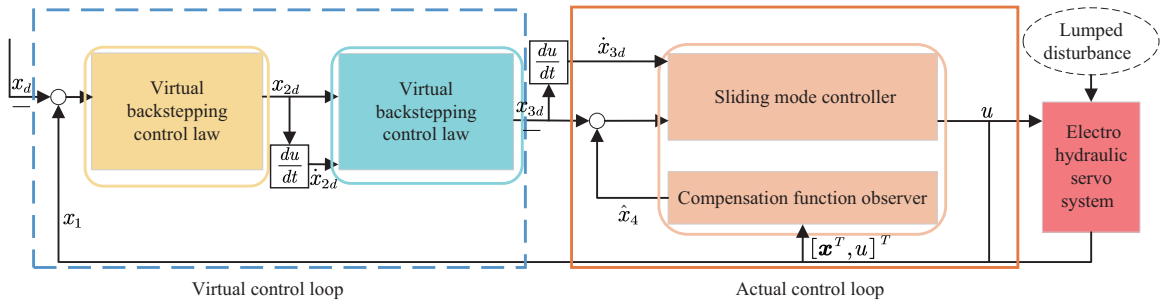

Figure 2. The structure of the proposed hierarchical control scheme based on CFO for EHSS

3.2. Design of Compensation Function Observer

To estimate disturbances with high accuracy, an CFO was recently proposed in [45]. Before employing this kind of obsever, expanding f_u in (4) as a new state, i.e., $x_4 = f_u$ yields

 doi:10.20944/preprints202409.0319.v1

$$\begin{cases} \dot{x}_1 = x_2, \\ \dot{x}_2 = x_3, \\ \dot{x}_3 = f_k + R_2 u + x_4, \\ \dot{x}_4 = \dot{f}_u. \end{cases} \tag{8}$$

Then, for (8), a fourth-order CFO is designed as

$$\begin{cases} \dot{z}_1 = z_2, \\ \dot{z}_2 = z_3, \\ \dot{z}_3 = f_k + R_2 u + L e_c + z_4, \\ \dot{z}_4 = \lambda L e_c, \\ \hat{f}_u = L e_c + z_4, \end{cases} \tag{9}$$

where z_i $(i = 1, 2, 3, 4)$ are the states of the CFO, $L = [l_3,\ l_2,\ l_1]$ is the vector of positive gain parameters, $e_c = [e_{c1},\ e_{c2},\ e_{c3}]^T = [x_1 - z_1,\ x_2 - z_2,\ x_3 - z_3]^T$, and λ is a positive filtering factor. Note that z_4 is a compensation term corresponding to x_4 in (8), but $z_4 \neq x_4$, which is the big difference from ESO and why the observer is called *compensation function observer* [48].

Define $\hat{x}_i$ as the estimates of x_i $(i = 1, 2, 3, 4)$ and $e_{ci} = x_i - \hat{x}_i$ are the estimation errors, then from (8) and (9), it obtains

$$\begin{cases} \hat{x}_1 = z_1, \\ \hat{x}_2 = z_2, \\ \hat{x}_3 = z_3, \\ \hat{x}_4 = \hat{f}_u = L e_c + z_4, \end{cases} \tag{10}$$

and

$$\begin{cases} \dot{e}_{c1} = \dot{x}_1 - \dot{z}_1 = e_{c2}, \\ \dot{e}_{c2} = \dot{x}_2 - \dot{z}_2 = e_{c3}, \\ \dot{e}_{c3} = \dot{x}_3 - \dot{z}_3 = f_k + R_2 u + x_4 - (f_k + R_2 u + L e_c + z_4) = e_{c4}. \end{cases} \tag{11}$$

Furthermore, the time derivative of (10) is obtained as

$$\begin{cases} \dot{\hat{x}}_1 = \hat{x}_2, \\ \dot{\hat{x}}_2 = \hat{x}_3, \\ \dot{\hat{x}}_3 = f_k + R_2 u + \hat{x}_4, \\ \dot{\hat{x}}_4 = \lambda l_3 e_{c1} + (l_3 + \lambda l_2) e_{c2} + (l_2 + \lambda l_1) e_{c3} + l_1 e_{c4}. \end{cases} \tag{12}$$

Subtracting (12) from (8) yields

$$\dot{E}_c = A_c E_c + B \dot{f}_u, \tag{13}$$

where $E_c = \left[e_c^T,\ e_{c4}\right]^T$ and

$$A_c = \begin{bmatrix} 0 & 1 & 0 & 0 \\ 0 & 0 & 1 & 0 \\ 0 & 0 & 0 & 1 \\ -\lambda l_3 & -l_3 - \lambda l_2 & -l_2 - \lambda l_1 & -l_1 \end{bmatrix}, B = \begin{bmatrix} 0 \\ 0 \\ 0 \\ 1 \end{bmatrix}. \tag{14}$$

Based on the above design procedure, the stability of the CFO and the convergence of the estimation errors are given in the following theorem.

 doi:10.20944/preprints202409.0319.v1

Theorem 1. *Consider the CFO designed in (9) for the EHSS with lumped unkown disturbance f_u. Suppose that f_u is fourth-order infinitesimal, if the gain parameters are chosen satisfying*

$$\begin{cases} l_1\left(\lambda l_1 + l_2\right) - \lambda l_2 - l_3 > 0, \\ l_1\left(\lambda l_1 + l_2\right)\left(\lambda l_2 + l_3\right) - \left(l_3 + \lambda l_2\right)^2 + \lambda l_1^2 l_3 > 0, \end{cases} \tag{15}$$

then the CFO is exponentially stable and the steady-state estimation error of the lumped disturbance is zero.

Proof. From (14), the characteristic equation of A_c is calculated as

$$s^4 + l_1 s^3 + \left(l_2 + \lambda l_1\right) s^2 + \left(l_3 + \lambda l_2\right) s + \lambda l_3 = 0, \tag{16}$$

and the Routh array of A_c is calculated as follows.

s^4	1	$l_2 + \lambda l_1 \quad \lambda l_3$
s^3	l_1	$l_3 + \lambda l_2 \quad 0$
s^2	$l_1\left(\lambda l_1 + l_2\right) - \lambda l_2 - l_3$	λl_3
s^1	$\frac{l_1(\lambda l_1 + l_2)(\lambda l_2 + l_3) - (l_3 + \lambda l_2)^2 + \lambda l_1^2 l_3}{l_1(\lambda l_1 + l_2) - \lambda l_2 - l_3}$	
s^0	λl_3	

According to the Routh-Hurwitz criterion, the system with A_c is exponential stable if all the elements in the first column of the Routh array are positive, i.e., inequalities (9) hold. Furthermore, since f_u is fourth-order infinitesimal, the fourth derivative f_u is zero, i.e., $\dddot{f}_u = 0$. Taking the time derivative of (13) three times yields

$$\dddot{E}_c = A_c \dddot{E}_c + B \dddot{f}_u = A_c \dddot{E}_c. \tag{17}$$

Because of the stability of A_c, it obtains

$$\lim_{t\to\infty} \dddot{E}_c = \lim_{t\to\infty} \left[\dddot{e}_c,\ \ddot{e}_{c4}\right] = \lim_{t\to\infty} \left[e_{c4},\ \dot{e}_{c4},\ \ddot{e}_{c4},\ \dddot{e}_{c4}\right] = 0, \tag{18}$$

i.e.,

$$\lim_{t\to\infty} e_{c4} = 0. \tag{19}$$

Therefore, the steady-state estimation error of the lumped disturbance is zero.

This completes the proof of Theorem 1. □

Remark 1. *It is worth noting that the CFO designed by Equation (9) has four gain parameters (l_1, l_2, l_3, λ), and the condition (15) is a little harsh for the parameter tuning of the CFO. However, a method of pole assignment can be employed to facilitate the search for parameters and ensure the stability of the system. The characteristic equation of the CFO can be rewritten as*

$$s^4 + l_1 s^3 + \left(l_2 + \lambda l_1\right) s^2 + \left(l_3 + \lambda l_2\right) s + \lambda l_3 = \left(s + \omega\right)^2 \left(s + 4\omega\right)^2 = 0, \tag{20}$$

where $\omega > 0$, is the bandwidth; $-\omega, -\omega, -4\omega, -4\omega$ are the poles of the CFO, having the relationship with the gain parameters as follows.

$$\begin{cases} l_1 = 10\omega, \\ l_2 + \lambda l_1 = 33\omega^2, \\ l_3 + \lambda l_2 = 40\omega^3, \\ \lambda l_3 = 16\omega^4. \end{cases} \tag{21}$$

 doi:10.20944/preprints202409.0319.v1

One solution of the above equations can be obtained as

$$l_1 = 10\omega, l_2 = 25\omega^2, l_3 = 20\omega^3, \lambda = \frac{4}{5}\omega. \tag{22}$$

Since ω is the only adjustable parameter, the selection of the gain parameters is quite simple. Generally speaking, a big bandwidth obtains a better observation performance. However, it may amplify the influence of high-frequency noise to the system, and even worse cause the instability of the control system. Therefore, the bandwidth should be suitablely selected by a trial and error method.

3.3. Design of Backstepping Sliding Mode Controller

Based on the CFO, backstepping technique integrated with sliding mode control is employed to design a controller to achieve the position tracking control objective.

Firstly, the tracking errors are defined as

$$\begin{cases} e_1 = x_1 - x_d, \\ e_2 = x_2 - x_{2d}, \\ e_3 = x_3 - x_{3d}, \end{cases} \tag{23}$$

where x_d is the desired trajectory, and x_{2d} and x_{3d} are virtual control laws to be designed step by step as follows.

Step 1: To stabilize e_1, the first Lyapunov function is chosen as:

$$V_1 = \frac{1}{2}e_1^2. \tag{24}$$

Based on (23), the derivative of V_1 is computed by

$$\dot{V}_1 = e_1\dot{e}_1 = e_1\left(\dot{x}_1 - \dot{x}_d\right) = e_1\left(e_2 + x_{2d} - \dot{x}_d\right). \tag{25}$$

To make $\dot{V}_1$ negative, the virtual control law x_{2d} is chosen as

$$x_{2d} = -k_1 e_1 + \dot{x}_d, \tag{26}$$

where k_1 is a positive design parameter. Substituting (26) into (25) yields

$$\dot{V}_1 = -k_1 e_1^2 + e_1 e_2. \tag{27}$$

Obviously, if $e_2 = 0$, then $\dot{V}_1 \leqslant 0$.

Step 2: Similarly, to stabilize e_2, the second Lyapunov function is chosen as:

$$V_2 = V_1 + \frac{1}{2}e_2^2. \tag{28}$$

Based on (23) and (27), the derivative of V_2 is obtained as

$$\dot{V}_2 = -k_1 e_1^2 + e_1 e_2 + e_2\left(e_3 + x_{3d} - \dot{x}_{2d}\right). \tag{29}$$

To make $\dot{V}_2$ negative, the virtual control law x_{3d} is chosen as

$$x_{3d} = -k_2 e_2 - e_1 + \dot{x}_{2d}, \tag{30}$$

where k_2 is a positive design parameter. Then, substituting (30) into (29) yields

$$\dot{V}_2 = -k_1 e_1^2 - k_2 e_2^2 + e_2 e_3. \tag{31}$$

 doi:10.20944/preprints202409.0319.v1

If $e_3 = 0$, then $\dot{V}_2 \leqslant 0$.

Step 3: To design a final actual control law for u, a sliding mode surface is chosen as

$$S = c_1 e_1 + c_2 e_2 + e_3, \tag{32}$$

where c_1 and c_2 are positive design parameters. Taking the time derivative of S and using (8) yields

$$\begin{aligned} \dot{S} =& c_1 \dot{e}_1 + c_2 \dot{e}_2 + \dot{e}_3 \\ =& c_1 \left(x_2 - \dot{x}_d\right) + c_2 \left(x_3 + k_1 \left(x_2 - \dot{x}_d\right) - \ddot{x}_d\right) + f_k + R_2 u + x_4 - \dot{x}_{3d} \\ =& (c_1 + c_2 k_1) x_2 + c_2 x_3 + x_4 + X_d + f_k + R_2 u \end{aligned} \tag{33}$$

where $X_d = -\left(c_1 + c_2 k_1\right) \dot{x}_d - c_2 \ddot{x}_d - \dot{x}_{3d}$ with

$$\dot{x}_{3d} = -\left(k_1 k_2 + 1\right) x_2 - \left(k_1 + k_2\right) x_3 + \left(k_1 k_2 + 1\right) \dot{x}_d + \left(k_1 + k_2\right) \ddot{x}_d + \dddot{x}_d. \tag{34}$$

The final Lyapunov function is chosen as

$$V_3 = \frac{1}{2} S^2 + V_2. \tag{35}$$

Based on (33), the derivative of V_3 is obtained as

$$\begin{aligned} \dot{V}_3 =& S\dot{S} - k_1 e_1^2 - k_2 e_2^2 + e_2 e_3 \\ =& S\left[(c_1 + c_2 k_1) x_2 + c_2 x_3 + x_4 + X_d + f_k + R_2 u\right] \\ & - k_1 e_1^2 - k_2 e_2^2 + e_2 (S - c_1 e_1 - c_2 e_2) \\ =& - k_1 e_1^2 - (k_2 + c_2) e_2^2 + e_2 S - c_1 e_1 e_2 \\ & + S\left[(c_1 + c_2 k_1) x_2 + c_2 x_3 + x_4 + X_d + f_k + R_2 u\right]. \end{aligned} \tag{36}$$

To make $\dot{V}_3$ negative, the actual control law u is designed as

$$u = -\frac{1}{R_2}\left[\left(c_1 + c_2 k_1\right) x_2 + c_2 x_3 + \hat{x}_4 + X_d + f_k + k_3 S\right], \tag{37}$$

where $\hat{x}_4$ is the estimate of the lumped disturbance f_u from the CFO in (9), and k_3 is a positive design parameter.

Summarizing the above results obtains the following theorem for the stability of the closed-loop control system.

Theorem 2. *Consider the EHSS with lumped disturbance described by (7). If the estimate of the lumped disturbance is employed from the CFO (9) and the design parameters are selected such that* $k_1 > \frac{c_1}{2} > 0$, $k_2 > \frac{c_1+1}{2} > 0$, $k_3 > \frac{1}{2}$, *then the backstepping sliding mode control laws (26), (30) and (37) guarantee that the closed-loop system is exponentially stable, and the tracking error signals converge to the origin.*

Proof. Consider the final Lyapunov function V_3 in (35). Substituting (37) into (36) yields

$$\dot{V}_3 = -k_1 e_1^2 - k_2 e_2^2 - k_3 S^2 + e_{c4} S + e_2 S - c_1 e_1 e_2. \tag{38}$$

According to Theorem 1, the estimation error of CFO converges to zero, i.e.,

$$\lim_{t \to \infty} e_{c4} = 0. \tag{39}$$

 doi:10.20944/preprints202409.0319.v1

In the sense of limiting, Equation (38) becomes

$$\begin{aligned}\dot{V}_3 &= -k_1 e_1^2 - k_2 e_2^2 - k_3 S^2 + e_2 S - c_1 e_1 e_2 \\ &\leq -k_1 e_1^2 - k_2 e_2^2 - k_3 S^2 + |e_2 S| + |c_1 e_1 e_2|.\end{aligned} \tag{40}$$

Using the Young's inequality for the last two terms of (40) obtains

$$|e_2 S| \leq \frac{1}{2} e_2^2 + \frac{1}{2} S^2, \qquad |c_1 e_1 e_2| \leq \frac{c_1}{2} e_1^2 + \frac{c_1}{2} e_2^2. \tag{41}$$

Substituting (41) into (40) yields

$$\begin{aligned}\dot{V}_3 &\leq -k_1 e_1^2 - k_2 e_2^2 - k_3 S^2 + |e_2 S| + |c_1 e_1 e_2| \\ &\leq -\left(k_1 - \frac{c_1}{2}\right) e_1^2 - \left(k_2 - \frac{c_1 + 1}{2}\right) e_2^2 - \left(k_3 - \frac{1}{2}\right) S^2.\end{aligned} \tag{42}$$

Rewriting inequality (42) in a compact form, it obtains

$$\dot{V}_3 \leq -\alpha_0 V_3, \tag{43}$$

where

$$\alpha_0 = \min\left(k_1 - \frac{c_1}{2},\, k_2 - \frac{c_1 + 1}{2},\, k_3 - \frac{1}{2}\right). \tag{44}$$

Selecting the design parameters $k_1 > \frac{c_1}{2} > 0$, $k_2 > \frac{c_1+1}{2} > 0$, $k_3 > \frac{1}{2}$ to ensure $\alpha_0 > 0$. Then, the solution of (43) is

$$V_3(t) \leq V_3(0)\, e^{-\alpha_0 t}, \tag{45}$$

which means that $V_3(t)$ converges exponentially to zero, i.e., as $t \to \infty$, $e_i (i = 1, 2, 3) \to 0$ and $S \to 0$. Therefore, the proposed CFO-based backstepping sliding model controller guarantees the stability of the closed-loop system of the EHSS, and the tracking errors converge to zeros.

This completes the proof of Theorem 2. □

4. Simulation Results and Analysis

To evaluate the effectiveness and efficiency of the proposed control scheme for the EHSS, two different working cases are simulated in the MATLAB/SIMULINK platform. The first case is to track an exponential trajectory with a relatively small f_d disturbance, while the second case is to track a sinusoidal position trajectory with a large f_d disturbance.

In all simulations, the system parameters such as coefficient of the viscous friction force B and leakage coefficient of the system C_t are assumed to be perturbed, which result in the uncertain parts ΔR_1 and ΔR_2 in (6) as: $\Delta R_1 = 0.1 R_1 \sin(\pi t)$ and $\Delta R_2 = 0.1 R_2 \sin(\pi t)$. The nominal physical parameters of the EHSS are listed in Table 1.

Table 1. Physical parameters of the electro-hydraulic servo system.

Parameters	Value	Parameters	Value
m (kg)	30	k_t ($m^3/s/V/Pa^{1/2}$)	1×10^{-8}
V_t (m^3)	2.398×10^{-5}	P_s (MPa)	10
β_e (Pa)	7×10^8	C_t ($m^3/s/Pa$)	3×10^{-12}
A (m^2)	9.047×10^{-4}	B ($N \cdot s \cdot m^{-1}$)	4×10^3

In addition, to illustrate the superiority of the proposed control approach, the following controllers are performed as comparison schemes.

 doi:10.20944/preprints202409.0319.v1

(1) **CFO-BSMC:** This is the proposed backstepping silding mode controller based on CFO presented in section 3. By trial and error, the parameters of the controller in (26), (30) and (37) are selected as $k_1 = 50, k_2 = 100, k_3 = 200, c_1 = 20$, c_2=2000. The bandwidth of the proposed CFO in Remark 1 is chosen as $\omega = 450$. Therefore, the gain parameters of the CFO are $l_1 = 4.5 \times 10^3, l_2 = 5.0625 \times 10^6, l_3 = 1.8225 \times 10^9, \lambda = 360$.

(2) **ESO-BSMC:** This is the backstepping silding mode controller based on the ESO proposed in [47]. To ensure a fair comparison, the parameters of the controller are chosen as the same as those in CFO-BSMC. In addition, the poles of the ESO are assigned as the same as CFO, having the characteristic equation $s^4 + l_{e1}s^3 + l_{e2}s^2 + l_{e3}s + l_{e4} = (s+\omega)^2 (s+4\omega)^2 = 0$, where $l_{e1}, l_{e2}, l_{e3}, l_{e4}$ are gain parameters of the ESO. The bandwidth is also chosen as $\omega = 450$, which results in $l_{e1} = 10\omega = 4.5 \times 10^3, l_{e2} = 33\omega^2 = 6.6825 \times 10^6, l_{e3} = 40\omega^3 = 3.645 \times 10^9, l_{e4} = 16\omega^4 = 6.561 \times 10^{11}$. Note that the maximum gainof the ESO is 240 times that of the CFO.

(3) **PID:** This is the well-known proportional-integral-derivative (PID) controller which has a wide range of application in industry [12]. By trial and error, the gain parameters of the PID controller are tuned as $k_p = 550, k_i = 1600, k_d = 0$. It is notable that larger gains would achieve better tracking performance. However, it also may cause instability under the influence of lumped disturbances. Therefore, the gain parameters are ultimately obtained by the trial and error method.

4.1. Case 1: Tracking an exponential-position trajectory

In this case, the desired trajectory is selected as an exponential signal whose initial state is zero and steady state is 0.005 m, i.e., $x_d = 0.005(1 - e^{-50t})$ m, and a time-varying sinusoidal external disturbance $f_d = 350 \sin(\pi t)$ N is imposed to the EHSS.

The simulation results of the EHSS under the three controllers are depicted in Figures 3–6, which record tracking performance, the tracking errors, the estimation performance for the lumped disturbance, and the control input, respectively.

As seen from Figure 3, the proposed controller achieves superior tracking control performance over the other two controller in the presence of parameter perturbations and time-varying sinusoidal disturbance. Specifically, by comparing the tracking error curves in Figure 4 during the transient and steady stages, it is evident that the tracking error of PID controller fluctuates more seriously than that of ESO-BSMC, as well as CFO-BSMC. The reason for this is that the lumped disturbance can be estimated and compensated by both ESO and CFO. Furthermore, by examining the estimation curves of ESO and CFO in Figure 5, it is apparent that CFO obtains a higher estimation accuracy than ESO under the same bandwidth. Figure 6 exhibits that the control signals of the three controller are smooth, continuous and bounded. This group of simulation results demonstrate the effectiveness and superiority of the proposed controller.

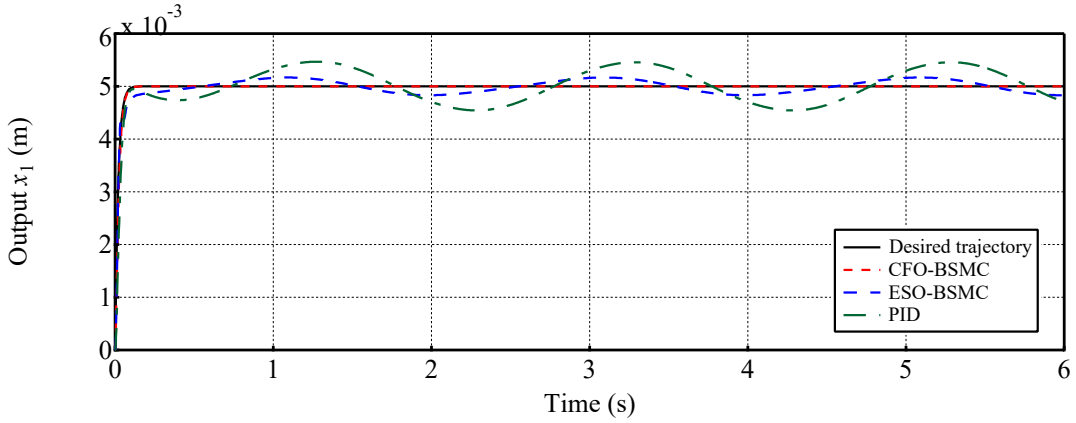

Figure 3. Comparison tracking performance in Case 1.

 doi:10.20944/preprints202409.0319.v1

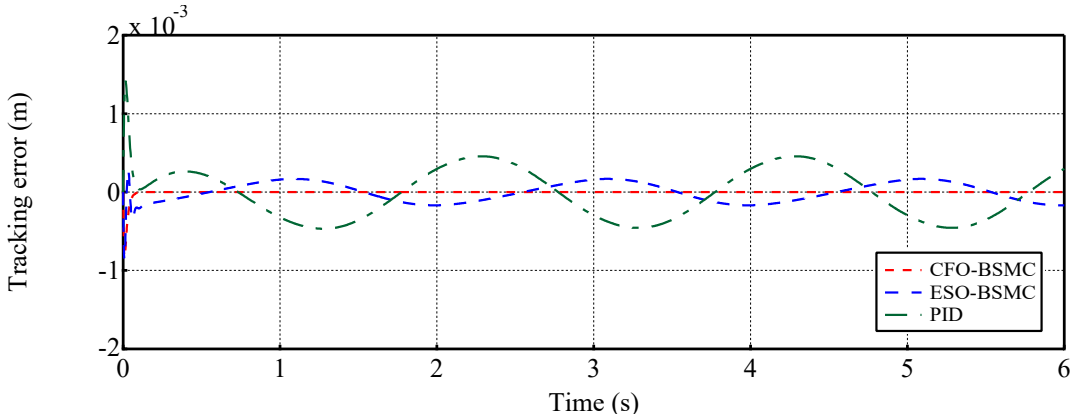

Figure 4. Comparison tracking errors in Case 1.

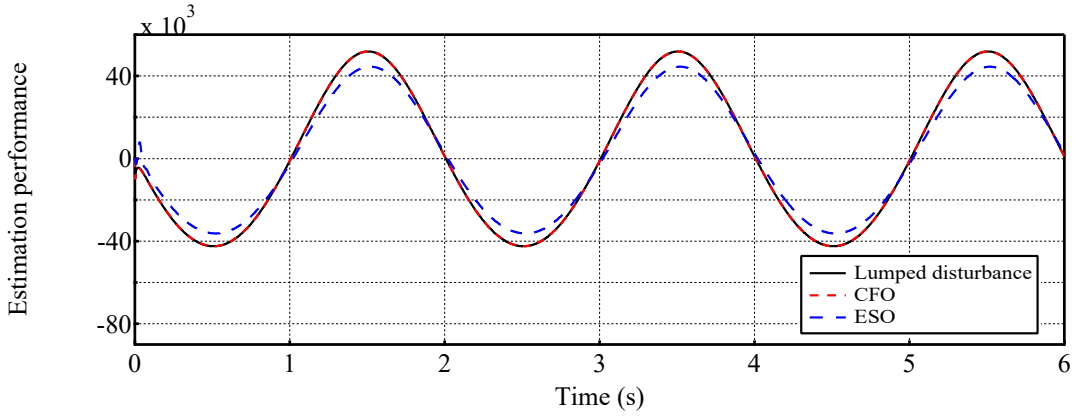

Figure 5. Comparison estimation performance for the lumped disturbance in Case 1.

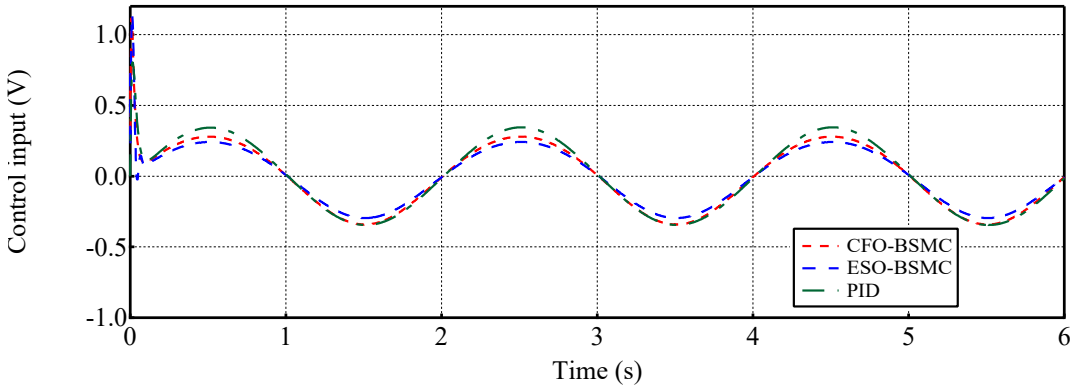

Figure 6. Comparison control input in Case 1.

4.2. Case 2: Tracking a sinusoidal position trajectory

To further test the tracking performance of the proposed controller, a smooth sinusoidal desired trajectory is employed as $x_d = 0.05\sin(\pi t)$ m. In addition, a large external disturbance is injected into the system to examine the robustness of the proposed controller. The disturbance is given as $f_d = 1000 + 3500\sin(\pi t)$ N, which is composed of a large constant load force and a large time-varying sinusoidal disturbance.

The output tracking performance of the three controllers is presented in Figure 7. As seen, the three controllers are able to drive the output of the EHSS close to the desired trajectory. Furthermore, a comparative result of tracking errors is shown in Figure 8, which indicates that the proposed CFO-BSMC has the smallest tracking error, followed by ESO-BSMC, and the worst is PID, which means the proposed controller achieves the best transient and steady state tracking performance.

 doi:10.20944/preprints202409.0319.v1

Moreover, by comparing the estimation performances between CFO and ESO in Figure 9, it is evident that the ESO presents a phase lag in estimating the disturbance, while the proposed CFO can estimate the disturbance accurately. The smooth, continuous and bounded control signals are shown in Figure 10.

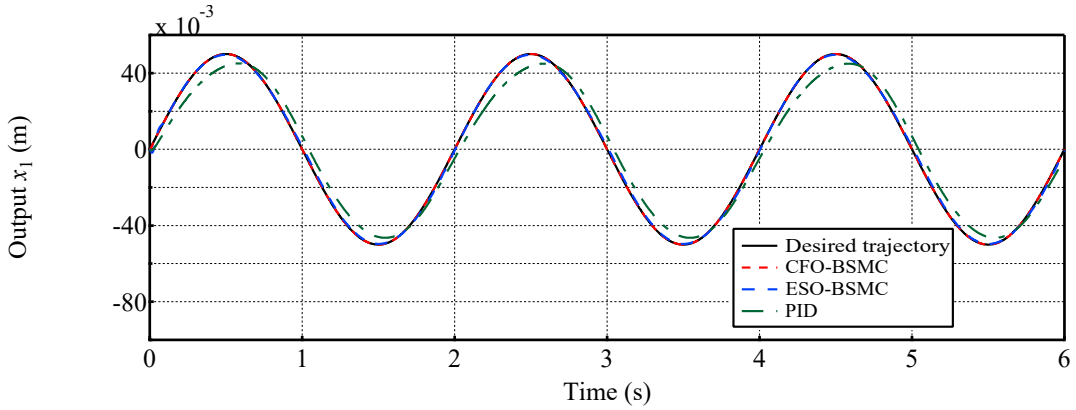

Figure 7. Comparison tracking performance in Case 2.

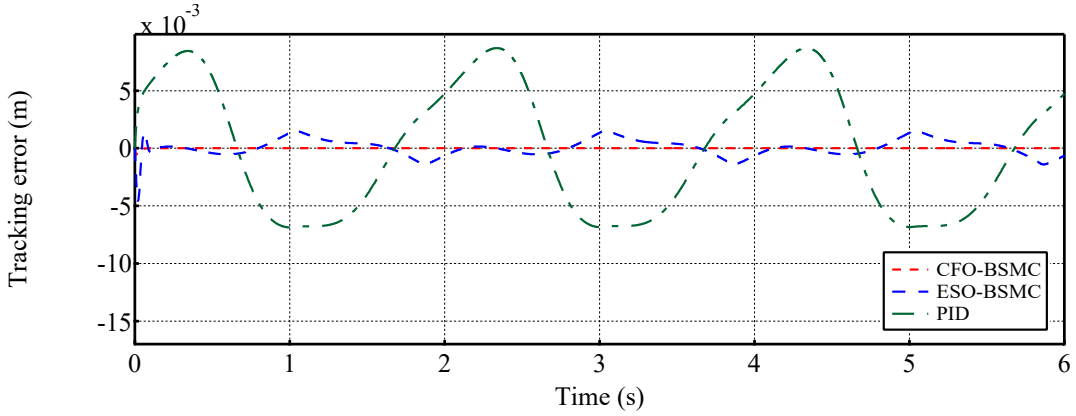

Figure 8. Comparison tracking errors in Case 2.

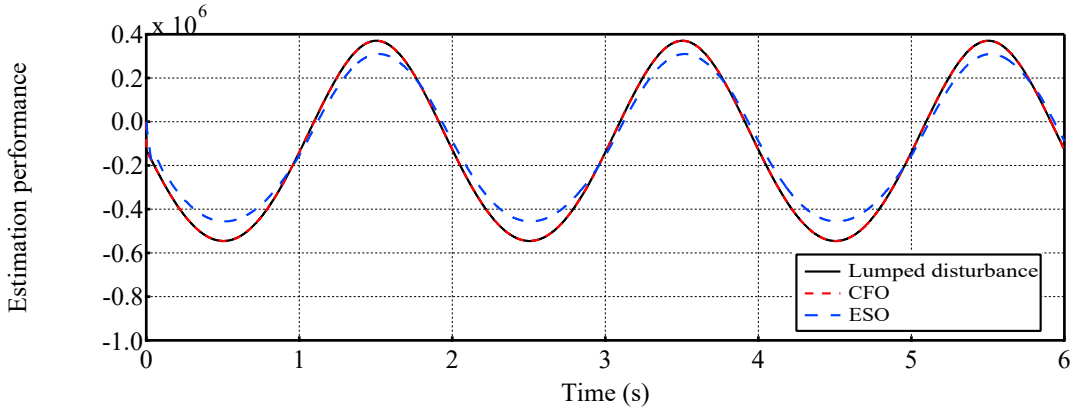

Figure 9. Comparison estimation performance for the lumped disturbance in Case 2.

Preprints.org (www.preprints.org) | NOT PEER-REVIEWED | Posted: 4 September 2024 doi:10.20944/preprints202409.0319.v1

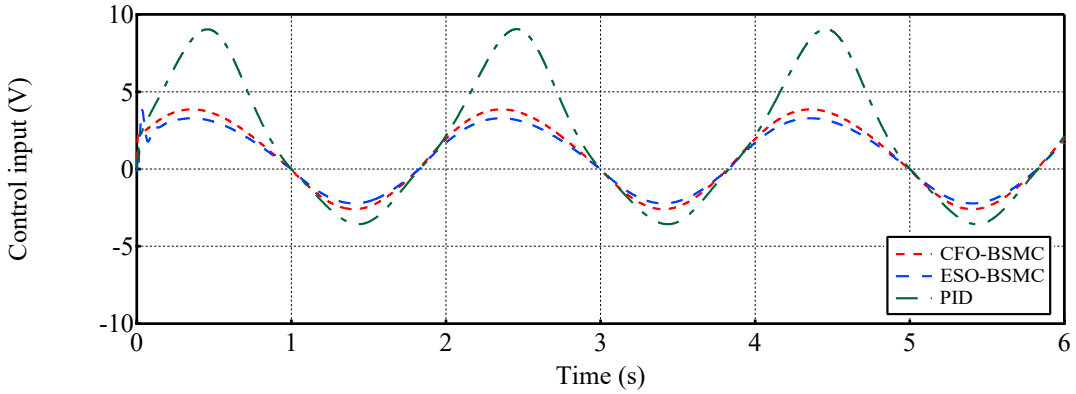

Figure 10. Comparison control input in Case 2.

In order to quantitatively analyze the control performance of the three controllers, three performance indices are introduced as follows [18]:

(1) Mean Absolute Error:

$$E_{MAE} = \frac{1}{N}\sum_{i=1}^{N}|e_1(i)|. \tag{46}$$

(2) Root Mean Square Error:

$$E_{RMSE} = \sqrt{\frac{1}{N}\sum_{i=1}^{N}(|e_1(i)| - E_{MAE})^2}. \tag{47}$$

(3) Integrated Time Absolute Error:

$$E_{ITAE} = \sum_{i=1}^{N} iT_s\,|e_1(i)|, \tag{48}$$

where T_s is the simulation step.

The obtained comparison results of the performance indices under the three controllers are presented in Table 2. It is clearly seen that all the indices of the proposed CFO-BSMC are the smallest among the three controllers. More specifically, compared with PID and ESO-BSMC, the mean absolute error E_{MAE} of the proposed CFO-BSMC is increased by 99.93% and 99.76%, and the the root mean square error E_{RMSE} is improved by 98.75% and 97.02%, respectively. These results verify that the proposed control approach achieves the best tracking accuracy. In addition, the integrated time absolute error E_{ITAE} is to weight the tracking error by time, which represents the system insensitivity to initial error and sensitivity to the steady error. Oblivious, the E_{ITAE} of the proposed controller is smallest, which means the proposed controller performs the best robustness against external disturbances.

Table 2. Comparison results of performance indices under different control methods.

Control methods	E_{MAE} (m)	E_{RMSE} (m)	E_{ITAE} (m)
PID ([12])	5.44800×10^{-3}	2.53951×10^{-3}	3.16250×10^{1}
ESO-BSMC ([47])	1.39804×10^{-3}	1.06401×10^{-3}	1.14442×10^{1}
CFO-BSMC (Proposed)	3.30503×10^{-6}	3.16826×10^{-5}	6.0590×10^{-3}

The simulation results in this group demonstrate that even in the presence of large external disturbances and system perturbations, the proposed control method can effectively estimate the lumped disturbance and compensate for its effect, achieving a high-precision tracking control for sinusoidal trajectory.

 doi:10.20944/preprints202409.0319.v1

5. Conclusions

In this paper, a novel CFO-based backstepping sliding model control method was proposed for the high-accuracy tracking control of EHSS in the presence of various uncertainties including nonlinearities, parameter perturbations and external disturbances. This method was founded upon the treatment of uncertainties as a lumped disturbance, on the basis of which a fourth-order CFO was presented to estimate the lumped disturbance accurately, and the estimate value was used for the compensation of the disturbance effect. A sliding model controller was developed by integrating the CFO into the backstepping design procedure. The stability of the closed-loop control system was rigorously proved by using Lyapunov theory, and all the tracking error signals were guaranteed to converge exponentially to the origin. Simulation results demonstrated that the proposed CFO delivered accurate estimate of the lumped disturbance, and compared with PID and ESO-based BSMC methods, the tracking accuracy was improved by 99.93% and 99.76% respectively.

It is worth mentioning that due to the limitations of working conditions and hardware equipments, there always exist some constraints on the input or output in the practical application of EHSS. In order to improve the practicality of the control method, it will be interesting to exploit a controller with the input or output constraint, which needs to investigate in the future work.

Author Contributions: Conceptualization, C.P.; methodology, Y.W.; validation, C.P. and Y.W.; investigation, Y.W. and Z.L.; writing—original draft preparation, Y.W.; writing—review and editing, C.P. and S.Y.; supervision, C.P. and Z.L.; project administration, C.P. and J.X. All authors have read and agreed to the published version of the manuscript.

Funding: This work is supported in part by: (i) National Natural Science Foundation of China (Grant No. 62173138); (ii) Guangdong Basic and Applied Basic Research Foundation (Grant No. 2020A1515011082 and No. 2019A1515010955); (iii) Hunan Provincial Natural Science Foundation of China (Grant No. 2022JJ30263 and No. 2023JJ40286).

Institutional Review Board Statement: Not applicable.

Informed Consent Statement: Not applicable.

Data Availability Statement: Not applicable.

Conflicts of Interest: Not applicable.

References

1. Bonchis, A.; Corke, P, I.; Rye, D, C.; Ha, Q, P. Variable structure methods in hydraulic servo systems control. *Automatica*. **2001**, *37*,589-595.
2. Vladimir, M.; Željko, Š.; Mario, E. Robust H_∞ position control synthesis of an electro-hydraulic servo system. *ISA Transactions*. **2010**, *49*,535-542.
3. Muhammad, B, N.; Wang, S, P. Optimization based on convergence velocity and reliability for hydraulic servo system. *Chinese Journal of Aeronautics*. **2009**, *22*,407-412.
4. Feng, H.; Ma, W.; Yin, C, B.; Cao, D, H. Trajectory control of electro-hydraulic position servo system using improved PSO-PID controller. *Automation in Construction*. **2021**, *127*,103722.
5. Chen, C.; Zhu, Z, H.; Hammadc, A. Automated excavators activity recognition and productivity analysis from construction site surveillance videos. *Automation in Construction*. **2020**, *110*,103045.
6. Keles, A.; Yildirim, M. Improvement of mechanical properties by means of titanium alloying to steel teeth used in the excavator. *Engineering Science and Technology, an International Journal* **2020**, *23*,1208-1213.
7. Dindorf, R.; Wos, P. Energy-Saving Hot Open Die Forging Process of Heavy Steel Forgings on an Industrial Hydraulic Forging Press. *Energies*. **2020**, *13*,1620.
8. Liu, Y.; Shu, Y.; Xu, Z.; Zhao, X.; Chen, M. Energy efficiency improvement of heavy-load hydraulic fine blanking press for sustainable manufacturing assisted by multi-stages pressure source system. *Proceedings of the Institution of Mechanical Engineers, Part B: Journal of Engineering Manufacture*. **2024**.
9. Xie, Q.; Zhang, Y.; Wang, T.; Zhu, S. Dynamic response prediction of hydraulic soft robotic arms based on LSTM neural network. Proceedings of the Institution of Mechanical Engineers, Part I, Journal of Systems and Control Engineering. *Electronics*. **2023**. *237*,1251-1265.

 doi:10.20944/preprints202409.0319.v1

10. Zhang, X, F.; Shi, G, L. Dual extended state observer-based adaptive dynamic surface control for a hydraulic manipulator with actuator dynamics. *Mechanism and Machine Theory*. **2022**, *169*,104647.
11. Chen, J, P.; Lu, B, C.; Fan, F.; Zhu, S, C.; Wu, J, X. A Nonlinear PID controller for electro-hydraulic servo system based on PSO algorithm. *Applied Mechanics and Materials*. **2012**, *141*, 157-161.
12. Karam, M, E.; Jiao, Z, X.; Zhang, H, Q. PID controller optimization by GA and its performances on the electro-hydraulic servo control system. *Chinese Journal of Aeronautics*. **2008**, *21*,378-384.
13. Kasprzyczak, L.; Macha, E. Selection of settings of the PID controller by automatic tuning at the control system of the hydraulic fatigue stand. *Mech Syst Signal Process*. **2008**, *22*, 1274–88.
14. Amiri, M.; Ramli, R.; Ibrahim, M. Hybrid design of PID controller for four DoF lower limb exoskeleton. *Appl Math Model*. **2019**, *72*, 17–27.
15. Honorine, A, M.; Ravinder, V.; Jean, P, K.; Christian, B. Feedback linearization-based position control of an electrohydraulic servo system with supply pressure uncertainty. *IEEE Transactions on Control Systems Technology*. **2012**, *20*, 1092-1099.
16. Aleksey, A, K. Feedback linearization of nonlinear singularly perturbed systems with state-dependent coefficients. *International Journal of Control*. **2020**, *18*, 1743-1750.
17. Angue, M, H.; Venugopal, R.; Kenne, J, P.; Belleau, C. Feedback linearization-based position control of an electrohydraulic servo system with supply pressure uncertainty. *IEEE Transactions on Control Systems Technology*. **2012**, *20*, 1092-1099.
18. Yao, J, Y.; Deng, W, X.; Sun, W, C. Precision motion control for electro-hydraulic servo systems with noise alleviation, a desired compensation adaptive approach. *IEEE/ASME Transactions on Mechatronics*. **2017**, *22*, 1859-1868.
19. Yang, G, C.; Y, J, Yao. High-precision motion servo control of double-rod electro-hydraulic actuators with exact tracking performance. *ISA Transactions*. **2020**, *103*, 266-279.
20. Feng, L, J.; Yan, H. Nonlinear adaptive robust control of the electro-hydraulic servo system. *Applied Sciences (Switzerland)*. **2020**, *10*, 4494.
21. Li, X.; Zhu, Z, C.; Rui, G, C.; Cheng, D.; Shen, G.; Tang, Y. Force loading tracking control of an electro-hydraulic actuator based on a nonlinear adaptive fuzzy backstepping control scheme. *Symmetry*. **2018**, *10*, 155.
22. Yan, C.; Xia J.; Liu X.; Yue H.; Li C. Adaptive backstepping control of high-order fully actuated nonlinear systems with event-triggered strategy. *Intelligence & Robotics* **2023**, 3(2), 176-89.
23. Zaare, S.; Soltanpour, M, R. Optimal robust adaptive fuzzy backstepping control of electro-hydraulic servo position system. *Transactions of the Institute of Measurement and Control*. **2022**, *44*, 1247-1262.
24. Li, J, F.; Ji, R, H.; Liang, X, L.; Ge, S, S.; Yan, H. Command filter-based adaptive fuzzy finite-time output feedback control of nonlinear electrohydraulic servo system. *IEEE Transactions on Instrumentation and Measurement*. **2022**, *71*, 1-10.
25. Niu, S, S.; Wang, J, Z.; Zhao, J, B.; Shen, W. Neural network-based finite-time command-filtered adaptive backstepping control of electro-hydraulic servo system with a three-stage valve. *ISA Transactions*. **2024**, *144*, 419-435.
26. Wan, Z, S.; Yue, L, W.; Fu, Y. Neural network based adaptive backstepping control for electro-hydraulic servo system position tracking. *International Journal of Aerospace Engineering*. **2022**, *2022*, 1-16.
27. Truong, H, V, A.; S, N.; Kim, S.; Kim, Y, W.; Chung, W, K. Backstepping-sliding-mode-based neural network control for electro-hydraulic actuator subject to completely unknown system dynamics. *IEEE Transactions on Automation Science and Engineering*. **2023**.
28. Dang, X.; Zhao, X.; Dang, C. Incomplete differentiation-based improved adaptive backstepping integral sliding mode control for position control of hydraulic system. *ISA transactions*. **2021**, *109*, 199-217.
29. Cao, Q, Y.; Su, X, Y. Generalized super-twisting backstepping sliding mode control for electro-hydraulic servo systems considering the coexistence of matched and mismatched uncertainties. *Applied Sciences*. **2023**, *13*, 4931.
30. Li, J.; Li, W.; Du, X. Adaptive backstepping sliding mode compensation control for electro-hydraulic load simulator with backlash links. *International Journal of Robust and Nonlinear Control*. **2024**, *34*, 8724-8743.
31. Wang, F.; Chen, G.; Liu, H.; Yan, G.; Zhang, T.; Liu, K.; Liu, Y.; Ai, C. Research on position control of an electro–hydraulic servo closed pump control system. *Processes*. **2022**, *10*, 1674.

 doi:10.20944/preprints202409.0319.v1

32. Feng, H.; Song, Q, Y.; Ma, S, L.; Ma, W.; Yin, C, B.; Cao, D, H.; Yu, H, F. A new adaptive sliding mode controller based on the RBF neural network for an electro-hydraulic servo system. *ISA Transactions*. **2022**. *29*, 472-484.
33. Chen, X, C.; Li, D.; Yang, X, B.; Yu, Y, C. Identification Recurrent Type 2 Fuzzy Wavelet Neural Network and L2-Gain Adaptive Variable Sliding Mode Robust Control of Electro-Hydraulic Servo System (EHSS). *Asian Journal of Control*. **2018**. *20*, 1480-1490.
34. Guo, X, P.; Wang, H, S.; Liu, H. Parameter adaptive based neural network sliding mode control for electro-hydraulic system with application to rock drilling jumbo. *International Journal of Adaptive Control and Signal Processing*. **2024**. *38*, 2554-2569.
35. Han, J, Q. From PID to Active Disturbance Rejection Control. IEEE Transactions on Industrial Electronics. **2009**. 56(3), 900-906.
36. He, C.; Sun H.; Wu Q.; Su Y.; Sun N. GPI observer-based active disturbance rejection control for a morphing quadrotor. *Intelligence & Robotics*. **2023**, 3(3): 274-87.
37. Zhuang, H, X.; Sun, Q, L.; Chen, Z, Q. Sliding mode control for electro-hydraulic proportional directional valve-controlled position tracking system based on an extended state observer. *Asian Journal of Control*. **2021**. *23*, 1855-1869.
38. Zou, Q. Extended state observer-based finite time control of electro-hydraulic system via sliding mode technique. *Asian Journal of Control*. **2022**. *24*, 2311-2327.
39. LAO, L, M.; Chen, P, Z. Adaptive sliding mode control of an electro-hydraulic actuator with a kalman extended state observer. *IEEE Access*. **2024**. *12*, 8970-8982.
40. Shen, W.; Shen, C. An extended state observer-based control design for electro-hydraulic position servomechanism. *Control Engineering Practice*. **2021**. *109*, 104730.
41. Meng, F, L.; Yan, H.; Li, J, F.; Liu, X. Finite-time backstepping control for electro-hydraulic servo system via extended state observer with perturbation estimation performance improvement. *Machines*. **2022**. *10*, 1163.
42. Liang, Q, K.; Cai, Y.; Song, J, C.; Wang, B, L. A novel ESO-based adaptive RISE control for asymptotic position tracking of electro-hydraulic actuator systems. *Transactions of the Institute of Measurement and Control*. **2024**. *46*, 1134-1145.
43. Yang, G, C. Dual extended state observer-based backstepping control of electro-hydraulic servo systems with time-varying output constraints. *Transactions of the Institute of Measurement and Control*. **2020**. *42*, 1070-1080.
44. Nguyen, M, H.; Ahn, K, K. Output feedback robust tracking control for a variable-speed pump-controlled hydraulic system subject to mismatched uncertainties. *Mathematics*. **2023**. *11*, 1783.
45. Qi, G, Y.; Li, X.; Chen, Z, Q. Problems of extended state observer and proposal of compensation function observer for unknown model and application in UAV. *IEEE Transactions on Systems, Man, and Cybernetics: Systems*. **2022**. *52*, 2899-2910.
46. Shao, X, L.; Wang, H, L. Back-stepping active disturbance rejection control design for integrated missile guidance and control system via reduced-order ESO. *ISA Transactions*. **2015**. *57*, 10-22.
47. Guo, B, Z.; Zhao, Z, L. On the convergence of an extended state observer for nonlinear systems with uncertainty. Systems & Control Letters. **2011**. 60(6), 420-430.
48. Qi, G, Y.; Deng, J, H.; Li, X.; Yu, X, C. Compensation function observer-based model-compensation backstepping control and application in anti-inference of quadrotor UAV. *Control Engineering Practice*. **2023**. *140*, 105633.
49. Qi, G, Y.; Hu, J, B.; Li, L, Y.;Li, K. Integral compensation cunction observer and its application to disturbance-rejection control of QUAV attitude. *IEEE Transactions on Cybernetics*. **2024**. *54*, 4088-4099.